

## Effect of Recoiled Oxygen on Characteristics of ITO Films Deposited by Ion Beam Sputtering

Satoshi IWATSUBO

Toyama Industrial Technology Center, 383 Takata, Toyama, Toyama 930-0866

Fax: 81-76-433-5466, e-mail: iwatsubo@itc.pref.toyama.jp

Characteristics of ITO films strongly depend on sputtering method. There is a possibility that bombardment of recoiled oxygen with high energy from target influences the characteristics. Ion beam sputtering has the advantage that substrates are separated from plasma, so that there are two ways to deposit the films by sputtering using mixed gas of oxygen. One exposes substrates to the oxygen as adsorptive gas ( $Ar+[O_2]$ ), and the other introduces the oxygen gas into ion source ( $Ar+O_2$ ) to generate the recoiled oxygen with high energy. So, the ITO films were deposited by sputtering in the two ways, and the dependence of the characteristics on the ratio of oxygen to total gas flow including argon  $R_{O_2/(Ar+O_2)}$  has been investigated. The composition of the films was almost same between them. But the structure, the resistivity  $\rho$  and the transmittance  $T$  of the films were remarkably different.  $\rho$  of the films for ( $Ar+O_2$ ) took the minimum value of  $6.5 \times 10^{-4} \Omega \text{ cm}$  at  $R_{O_2/(Ar+O_2)}$  around 0.33.  $T$  for ( $Ar+O_2$ ) was higher than that for ( $Ar+[O_2]$ ). It was found that bombardment of the recoiled oxygen enhanced  $T$  without the increase of  $\rho$ .

Key words: ITO, ion beam, sputtering, thin film, oxygen, argon

### 1. INTRODUCTION

Transparent conductive films, represented by  $\text{In}_2\text{O}_3$ : Sn (ITO) and ZnO are widely used as electrodes for flat panel displays, solar cells and electroluminescence (EL) devices.<sup>11-12)</sup> Especially, ITO films are prepared by various methods such a chemical vapor deposition (CVD), evaporation, sputtering. Recent technology requires a preparation of ITO films with high quality at low temperature to use a top electrode on sensitive materials such as organic. Among these methods, ITO films with low resistivity are frequently deposited by rf magnetron sputtering<sup>13)</sup>, dc magnetron sputtering under low sputtering voltage<sup>14)</sup> and FTS of plasma free process<sup>15)</sup>. For the conventional plasma sputtering, the substrates are near the plasma in the apparatus, so that the films are always bombarded by recoiled argon, oxygen and plasma. It is known that energy of the recoiled argon and oxygen is considerably high. So, there is a possibility that bombardment of the recoiled oxygen strongly influences the characteristics. In addition, adsorption in atmosphere of introduced gas also occurs.<sup>16)</sup> So, to deposit ITO films with high quality, the effect of the recoiled and adsorptive oxygen must be clear.

Ion beam sputtering has the advantage that substrates are separated from the plasma. For

this reason, there are two ways for introduced gas on ion beam sputtering. One is sputtering using adsorptive oxygen in atmosphere by oxygen introduced into chamber, and the other is sputtering using oxygen recoiled from target by oxygen introduced into ion source. In this study, the ITO films were deposited by the ion beam sputtering in their ways, and the dependence of the characteristics on the ratio in flowing rate of oxygen gas to mixture gas including argon  $R_{O_2/(Ar+O_2)}$  has been investigated.

### 2. EXPERIMENTAL PROCEDURE

Figure 1 shows the schematic illustration of the ion beam sputtering apparatus used in this study and the introduction ways of the gas. Kaufman-type ion source was used. Specimen films were deposited on water-cooled glass substrates by ion beam sputtering using the ITO ( $\text{In}_{35}\text{Sn}_5\text{O}_{60}$ ) target. The residual gas pressure in the chamber was lower than  $6 \times 10^{-5}$  Pa. Argon gas of 99.999% in purity for sputtering was introduced into the ion source at flowing rate of 2 sccm, so that argon pressure was as high as 3.6 mPa. Oxygen gas was introduced by the two ways into the chamber ( $Ar+[O_2]$ ) and into the ion source ( $Ar+O_2$ ), as shown Fig. 1 (a) and (b), respectively. The flowing rate was varied in the range between 0.125 and 16 sccm. The

mean free path of oxygen was longer than the distance of target and substrate at the flowing rate of 16 sccm. So, the recoiled oxygen from the target directly arrives at the substrates. The sputtering voltage and current were fixed at 1200 V and 30 mA, respectively. Film thickness was 500 nm. The composition and the crystal structure were analyzed by XPS and X-ray diffractometry. The morphology in the films was observed by SEM. The resistivity  $\rho$  was measured using by a four probe method. Concentration  $N_C$  and mobility of free electron  $\mu$  were estimated from Hall measurements by Van del Pauw method. The optical transmission spectra of the films were measured by a spectroscopy in the wave range from 300 to 2500 nm.

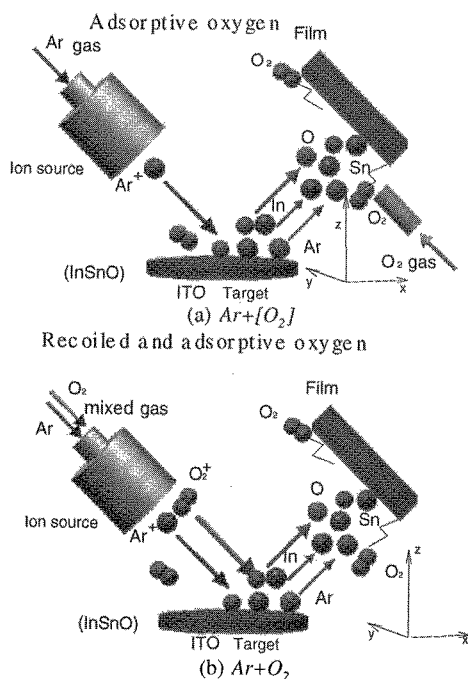


Fig. 1. Schematic illustration of ion beam sputtering apparatus used in this study and introduction ways of gas.

### 3. RESULTS AND DISCUSSION

#### A. Simulation of recoiled argon and oxygen

For a sputtering, it is known that energy and amount of ions recoiled from target are closely related to mass numbers of target atoms and sputtering ions. The mass numbers of indium, tin, oxygen and argon are 114.8, 118.7, 16 and 39.9, respectively. Oxygen and argon as sputtering gas are much smaller than the elements of the target. Therefore, there is a high possibility that the films sputtered using argon or oxygen introduced into ion source are bombarded by a large amount of recoiled argon or oxygen with high energy. So, the energy of oxygen and argon recoiled from ITO target was estimated by Monte-Carlo simulation TRIM<sup>[7]</sup>. The calculations are based on a direct Monte-Carlo method applied to an amorphous ITO target. Figures 2 show the schematic

layout of the apparatus and the angular distributions in energy of the recoiled oxygen. The ionized oxygen gas in the ion source is almost in  $O_2^+$ .<sup>[8]</sup> So, on the assumption that atomic collisions at the target detach O from  $O_2^+$ , the acceleration energy of O is half. Therefore, the simulation for the recoiled oxygen was carried out at acceleration voltage of 600 V and 100000 events. Both of the incident angle of the sputtering ion beam to target plane and the angle of the substrate from target plane are equal to 45°. The small dot in the figure corresponds to an oxygen atom. The length and the direction to the dot indicate the energy and the angle projected in the plane included the three points of the ion source, the target and the substrate, respectively. In Fig. 2, a large amount of the oxygen is reflected from the ion source in the direction of the target plane to the substrate. The substrate was bombarded by the recoiled oxygen with the high energy up to 500 eV. Taking statistics of the oxygen arriving at the substrate, the average energy  $\langle E_O \rangle$  was 202 eV. Similarly, the average energy for the recoiled argon  $\langle E_{Ar} \rangle$  was 280 eV at acceleration voltage of 1200 V. These results indicate that bombardment by the recoiled oxygen and argon is very serious for the growing films. So,  $R_{O2/(Ar+O2)}$  for  $Ar+[O_2]$  shows the only variation of the amount of adsorptive oxygen, and the constant bombardment by the recoiled argon.  $R_{O2/(Ar+O2)}$  for  $Ar+O_2$  shows the variation of the ratio of the recoiled oxygen to the sum of the recoiled argon and oxygen, and the variation of adsorptive oxygen for  $Ar+[O_2]$ .

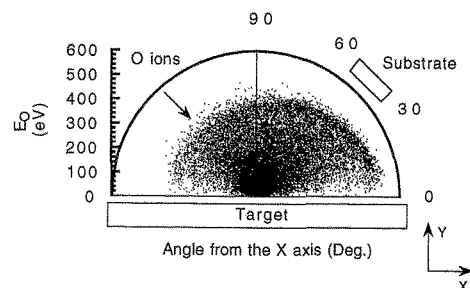


Fig. 2. Angular distribution of recoiled oxygen.

#### B. Experimental results

Taking effect of the recoiled oxygen and argon into consideration, the composition of the deposited films may change by the bombardment. So, the content of In, O and Sn was measured using XPS spectra of In3d5/2, O1s and Sn 3d5/2. Figure 3 shows the  $R_{O2/(Ar+O2)}$  dependence of the In, O and Sn content ( $C_{In}$ ,  $C_O$  and  $C_{Sn}$ ). The content of the films deposited by the two ways of  $Ar+[O_2]$  and  $Ar+O_2$  was almost same.  $C_{In}$  of the films decreased from 40 to 38 at.% as  $R_{O2/(Ar+O2)}$  increased.  $C_O$  increased decreased from 55 to

59 at.%.  $C_{Sn}$  was almost constant at 4.5 at.%. This result indicates that the amount of the adsorptive oxygen closely depended on  $C_O$ . The value of  $C_{In}$  of the films was higher than that of the target.

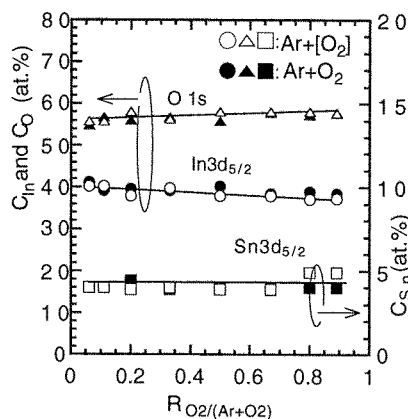


Fig. 3  $R_{O_2/(Ar+O_2)}$  dependence of In, O and Sn content ( $C_{In}$ ,  $C_O$  and  $C_{Sn}$ ).

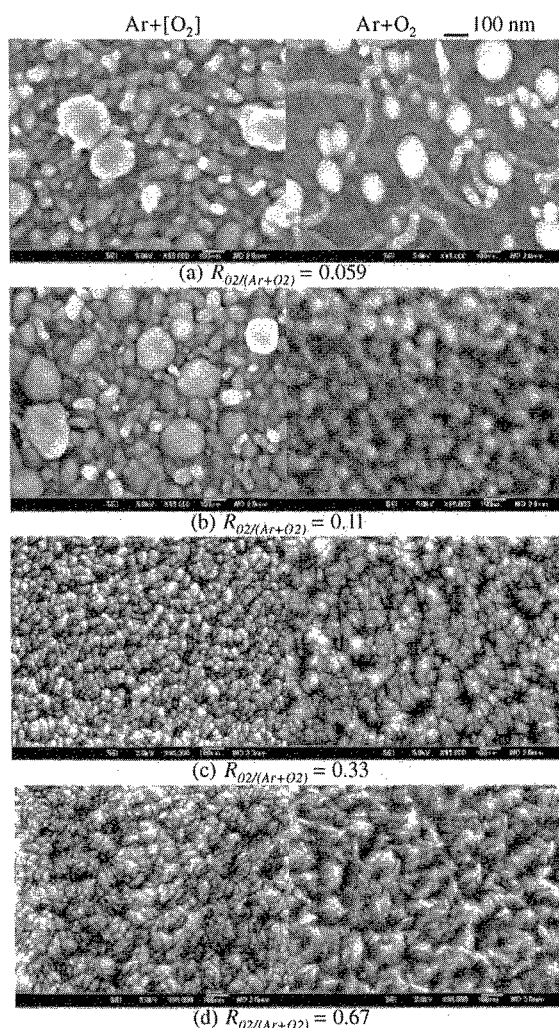


Fig. 4 Typical SEM images of ITO films deposited by two ways.

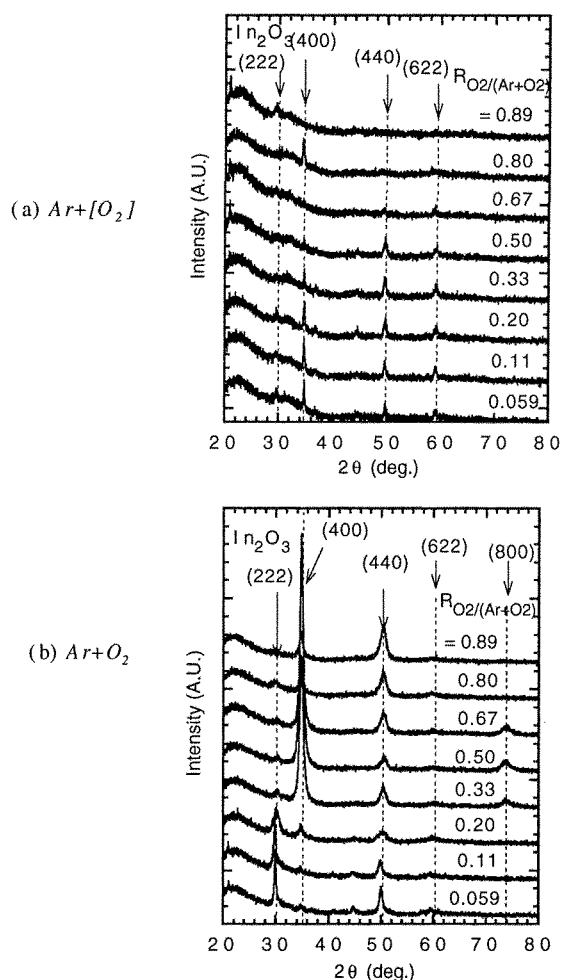


Fig. 5 X-ray diffraction patterns of ITO films as a parameter of  $R_{O_2/(Ar+O_2)}$ .

Figure 4 shows the typical SEM images of the ITO films deposited by the two ways. The left and right images in the figure shows ones deposited by  $Ar+[O_2]$  and  $Ar+O_2$ , respectively. The morphology of film surface was very different between them. For  $Ar+[O_2]$ , the large grains up to 200 nm in a width and the small grains appeared at  $R_{O_2/(Ar+O_2)}$  below 0.11. At  $R_{O_2/(Ar+O_2)}$  of 0.33, the grain size was drastically small. At  $R_{O_2/(Ar+O_2)}$  above 0.33, the grain size was decreased with an increase of  $R_{O_2/(Ar+O_2)}$ . For  $Ar+O_2$ , the large grains only appeared at  $R_{O_2/(Ar+O_2)}$  of 0.059. At  $R_{O_2/(Ar+O_2)}$  above 0.33, the grain size increased with an increase of  $R_{O_2/(Ar+O_2)}$  and was longer than that of  $Ar+[O_2]$ .

Figure 5 shows the CuK $\alpha$  X-ray diffraction patterns of the ITO films as a parameter of  $R_{O_2/(Ar+O_2)}$ . For  $Ar+[O_2]$ , X-ray diffraction peaks of (222), (400), (440) and (622) planes of  $In_2O_3$  appeared. At  $R_{O_2/(Ar+O_2)}$  of 0.67, peaks of (440) and (622) plane vanished. For  $Ar+O_2$ , the peak intensity of (222) planes was higher than that for  $Ar+[O_2]$ . At  $R_{O_2/(Ar+O_2)}$  above 0.33, the high peak of (400) plane appeared. The bombardment of the recoiled oxygen promoted the crystallization and enlarged the grain size.

Figure 6 shows the  $R_{O_2/(Ar+O_2)}$  dependence of resistivity  $\rho$ .  $\rho$  of both films took the minimum values at  $R_{O_2/(Ar+O_2)}$  of 0.33.  $\rho$  for  $Ar+O_2$  was the lowest value of  $6.5 \times 10^{-4} \Omega\text{cm}$ .  $\rho$  for  $Ar+[O_2]$  changed in the range between  $7.4 \times 10^{-4}$  and  $1.0 \times 10^{-5} \Omega\text{cm}$ .  $\rho$  for  $Ar+O_2$  widely changed and drastically increased at  $R_{O_2/(Ar+O_2)}$  above 0.67.

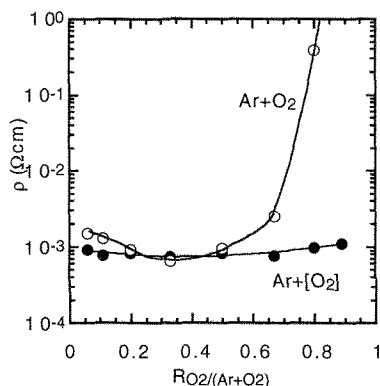


Fig. 6  $R_{O_2/(Ar+O_2)}$  dependence of resistivity  $\rho$ .

Figure 7 shows the  $R_{O_2/(Ar+O_2)}$  dependence of the carrier concentration  $N_C$  and the carrier mobility  $\mu$ . For  $Ar+[O_2]$ ,  $N_C$  decreased from  $1.5 \times 10^{22}$  to  $9.0 \times 10^{20} \text{cm}^{-3}$  with an increase of  $R_{O_2/(Ar+O_2)}$  in the range between 0.057 and 0.33.  $N_C$  gradually decreased at  $R_{O_2/(Ar+O_2)}$  above 0.33. For  $Ar+O_2$ ,  $N_C$  was constant at  $R_{O_2/(Ar+O_2)}$  below 0.33 and drastically decreased from  $1.0 \times 10^{21}$  to  $1.0 \times 10^{19} \text{cm}^{-3}$  at  $R_{O_2/(Ar+O_2)}$  above 0.50.  $\mu$  of both films increased in the range between 0.059 and 0.50. At  $R_{O_2/(Ar+O_2)}$  above 0.50,  $\mu$  was almost constant.  $\mu$  for  $Ar+O_2$  are higher than that for  $Ar+[O_2]$ . These results indicate that adsorptive oxygen was required to increase  $\mu$ , the recoiled oxygen increased  $\mu$  owing to the improvement of the crystallization and decreased  $N_C$  and the recoiled argon increased  $N_C$ .

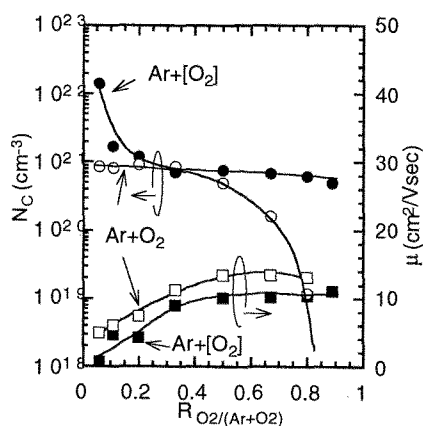


Fig. 7  $R_{O_2/(Ar+O_2)}$  dependence of carrier concentration  $N_C$  and carrier mobility  $\mu$ .

Figure 8 shows the typical transmittance  $T$  spectra of the ITO films as a parameter of  $R_{O_2/(Ar+O_2)}$ .  $T$  of both

films deposited at  $R_{O_2/(Ar+O_2)}$  of 0.056 was lower than 5%.  $T$  increased to 75 % for  $Ar+O_2$  and 95 % for  $Ar+[O_2]$  with an increase of  $R_{O_2/(Ar+O_2)}$ .  $T$  of films for  $Ar+O_2$  was higher than that for  $Ar+[O_2]$ .  $T$  of the films with minimum  $\rho$  were 65 for  $Ar+O_2$  and 75 % for  $Ar+O_2$ .

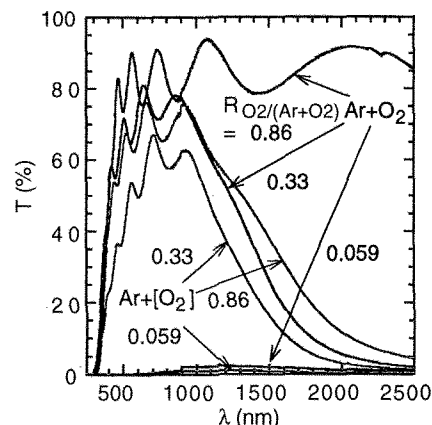


Fig. 8 Transmittance  $T$  spectra of ITO films as a parameter of  $R_{O_2/(Ar+O_2)}$ .

#### 4. CONCLUSION

The ITO films were deposited by the ion beam sputtering in the two ways as a parameter of  $R_{O_2/(Ar+O_2)}$ . One is to use the adsorptive oxygen in the atmosphere ( $Ar+[O_2]$ ), the other is mainly to use the recoiled oxygen with the average energy of 202 eV ( $Ar+O_2$ ). The composition of both films was almost same. The recoiled oxygen enlarged the grain size, promoted the crystallization and increased  $\mu$ .  $\rho$  of films with bombardment of the recoiled oxygen took the minimum value of  $6.5 \times 10^{-4} \Omega\text{cm}$  at  $R_{O_2/(Ar+O_2)}$  around 0.33.  $T$  of the films with bombardment of the recoiled oxygen was higher than that of adsorptive oxygen. Consequently, the recoiled oxygen for the ion beam sputtering widely changed the characteristics of the films, the bombardment enhanced the optical transmittance without the increase of the resistivity.

#### References

- [1] K. L. Chopra, S. Major and D. K. Pandya, *Thin Solid Films*, **102**, 1 (1983)
- [2] I. Hamberg and C. G. Granqvist, *J. Appl. Phys.*, **60**, R123 (1986)
- [3] K. Sreenivas, T. S. Rao and A. Mansingh, *J. Appl. Phys.*, **57**, 384 (1985)
- [4] R. Ohki and Y. Hoshi, Technical Report of IEICE (CPM99-91), 27, (1999) in Japanese
- [5] Y. Hoshi, Technical Report of IEICE (CPM86-54), 159, (1986) in Japanese
- [6] S. Iwatsubo and M. Naoe, *Vacuum*, **66**, 251, (2002)
- [7] J. P. Biersack, W. Eckstein, *Appl. Phys. A*, **34**, 73 (1984)
- [8] D. Vechten, G. K. Hubler, E. P. Donovan, and F. D. Correl, *J. Vac. Sci. Technol. A* **8**(2), 821, (1990)